Journal of the European Ceramic Society 19 (1999) 1105–1109

PII: S0955-2219(98)00383-5
0955-2219/99/$ - see front matter

$K_2Sr_4Nb_{10}O_{30}$-based Dielectric Ceramics having the Tetragonal Tungsten Bronze Structure and Temperature-stable High Permittivity

B. Tribotté,[a]* J. M. Haussonne[b] and G. Desgardin[a]

[a]Laboratoire CRISMAT, ISMRA, 6 bd Maréchal Juin, 14050 Caen Cedex, France
[b]LUSAC, Laboratoire 4233, Site Universitaire, 50130 Octeville, France

Abstract

This study concerns $K_2Sr_4Nb_{10}O_{30}$-based (KSN) dielectric ceramics, having the tetragonal tungsten bronze structure (TTB), which display a high permittivity and flat $\varepsilon'_r = f(T)$ *curves meeting the X7R specification. The series* $K_2Sr_4(Mg_xNb_{10-x})O_{30-(3/2)x}$ *exhibit these properties, as well as* $K_2Sr_4Nb_{9.78}O_{29.45}$ *and* $K_2(Sr_{3.25}Pb_{0.75})Nb_{9.78}O_{29.45}$ *when sintered with MgO or* ZrO_2*. Both X-ray and electron diffraction reveal the former composition to be a single phase material with the TTB structure. In this material, the presence of disorder, resulting from a large variation in the local K/Sr ratio and the presence of Zr on the octahedral niobium sites, is primarily responsible for the X7R* $\varepsilon'_r = f(T)$ *curve with* $\varepsilon'_{r,25°C} = 5000$*. © 1999 Elsevier Science Limited. All rights reserved*

Keywords: TTB structure, dielectric properties, niobates, capacitors.

1 Introduction

Dielectric materials meeting the X7R specification ($\Delta C/C_{25°C} = \pm 15\%$ between −55 and 125°C) having a high permittivity, are still investigated in order to increase the capacitance per unit volume of multilayers capacitors and to confer a high-temperature stability of ε'_r. As well as numerous works based on perovskites,[1,2] Boufrou *et al.*[3,4] mixed $Pb(Mg_{1/3}Nb_{2/3})O_3$ and the TTB phase $K_2Sr_4Nb_{10}O_{30}$ or different TTB phases, to obtain $\varepsilon'_r = f(T)$ curves with a flat profile and a permittivity above 5000. In the present study, we report the synthesis of other $K_2Sr_4Nb_{10}O_{30}$-based compositions with the TTB structure, characterised by flat $\varepsilon'_r = f(T)$ curves and a high permittivity. Previous results have pointed out the interest of $K_2Sr_4Nb_{10}O_{30}$ (KSN), in relation with the flat profile of the $\varepsilon'_r = f(T)$ curves.[5] Effectively, a wide range of compositional variation favours greater disorder of the cations on the different sites of the TTB structure: K^+ and Sr^{2+} are found in the pentagonal and tetragonal tunnels and Nb^{5+} is disordered with Mg^{2+} over the octahedral sites.

2 Experimental Procedure

The reagent mixture of Nb_2O_5,K_2CO_3,$SrCO_3$ and PbO was wet-attrition milled in ethanol. The calcination was performed in air at 1200°C for 4 h with a heating/cooling rate of 150°C/h. The sintering of the pressed samples (100 MPa) was performed at 1300°C for 2 h (150°C/h). The calcined powders and the sintered ceramics were characterised by XRD using a Guinier camera. HREM study was performed with a Topcon 002B, having an acceleration voltage of 200 kV and a point resolution close to 1·8Å ($C_S = 0{\cdot}4$ mm). The microstructures were studied by SEM using a Philips XL30 FEG, equipped with EDS detector (Oxford Link Isis 300). The dielectric characteristics of the sintered disks, whose faces were painted with an In-Ga alloy to make a capacitor, were performed at 1 kHz between −60 and 150°C.

3 Results and Discussions

The solid solution $K_2Sr_4(Mg_xNb_{10-x})O_{30-(3/2)x}$ was synthesised, without cationic charge balance, to see

*To whom correspondence should be addressed. Fax: + 33-02-31951600; e-mail: ceram@crismat.ismra.fr

the effect of Mg.[5] Flat $\varepsilon'_r = f(T)$ curves were obtained but the presence of Mg- and Nb-rich secondary phases, were detrimental to the dielectric properties. The present work concerns, therefore, the nominal compositions $K_2Sr_4Nb_{10}O_{30-(5/2)x}$ and particularly $x = 0{\cdot}22$ ($K_2Sr_4Nb_{9{\cdot}78}O_{29{\cdot}45}$), whose dielectric properties are better, especially when magnesium is added as a sintering agent.

3.1 $K_2Sr_4Nb_{9{\cdot}78}O_{29{\cdot}45}$ sintered with MgO

The synthesis of the nominal composition $K_2Sr_4Nb_{9{\cdot}78}O_{29{\cdot}45}$ leads to a single phase with the TTB structure, after calcination and sintering. Sintered samples, even at 1400°C, are friable because of the presence of macrocracking in a matrix of micron-sized grains. A study showed that a TTB phase with partially occupied tunnels and a K/Sr ratio different from 0·5 seems to be formed from the nominal composition.[5]

To improve densification, magnesium is used as a sintering agent instead of a structural agent. MgO is added in low content to the calcined powder before sintering (0·25, 0·5 and 1 wt%). The porosity of the corresponding ceramics decreases dramatically and interesting dielectric properties are obtained (Fig. 1). The dielectric losses decrease when the MgO content increases and the principal effect of MgO in the $\varepsilon'_r = f(T)$ curves is the presence of a maximum at low temperature for 1%. The interesting point is a 'tilt' effect between 0·25 and 1% due to the presence of maxima at low and high temperature, involving that the intermediate curve exhibits a flat profile compatible with the X7R class. The presence of Mg- and Nb-rich secondary phases in the sintered samples, detected by SEM, must decrease the average level of ε'_r and the dielectric characteristics are similar to those obtained in the compositions $K_2Sr_4(Mg_xNb_{10-x})O_{30-(3/2)x}$.[5]

The presence of Mg on the octahedral sites, normally occupied by Nb^{5+}, increases the ionic character of the metal-oxygen bonds (therefore lowering the Curie temperature) and contributes to the flat temperature profile of ε'_r, due to disorder. Mg^{2+} has an electronegativity lower than Nb^{5+} and a higher ionic radius ($r(Mg^{2+}) = 0{\cdot}72$ Å and $r(Nb^{5+}) = 0{\cdot}64$ Å) resulting in a distortion of the octahedra of the TTB structure. These aspects have already been reported for different substitutions in perovskite and TTB structures.[6]

3.2 $K_2Sr_4Nb_{9{\cdot}78}O_{29{\cdot}45}$ sintered with other agents

Considering cation size and electronegativity, four cations were selected as sintering agent and the same mole% was added in all cases to give weight percentages: 2·74% of Ta_2O_5, 0·86% of Sc_2O_3, 1·52% of ZrO_2 and 2·14% of CeO_2, c.f 0·5 wt% of MgO previously used.

XRD patterns of the 1300°C-2 h sintered disks show a TTB phase, isotypic of KSN; a splitting of the 620-002 lines for ZrO_2 and CeO_2 indicates an octahedral distortion. We could suppose that Zr and Ce partially occupy the octahedral sites. In fact, the Ce^{4+} cation seems to preferentially

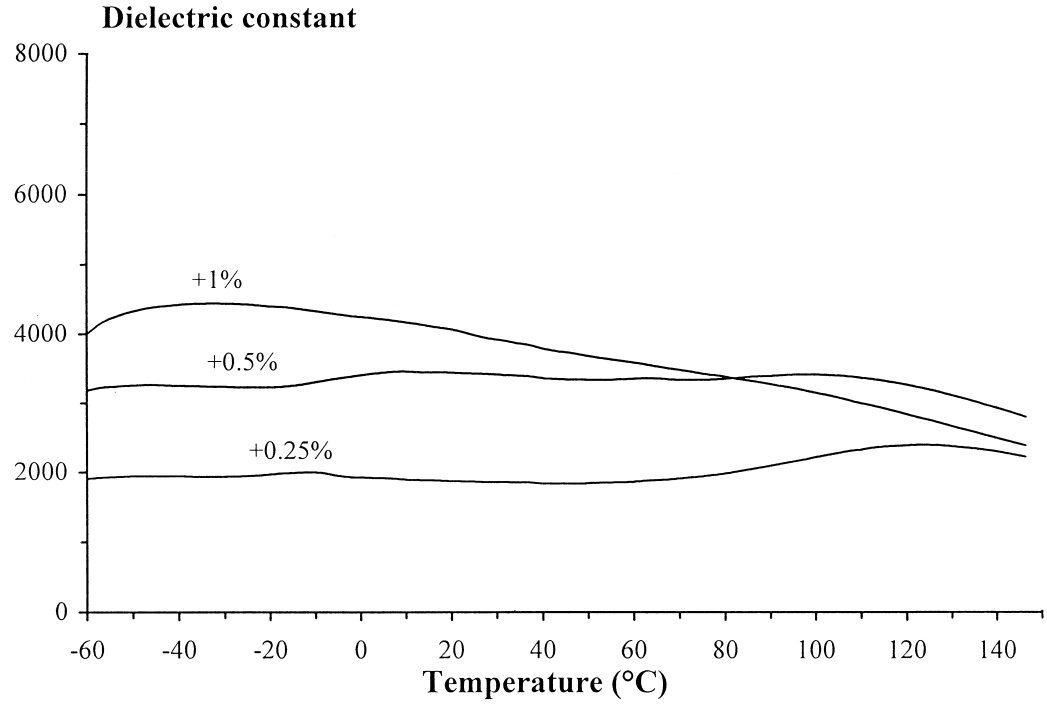

Fig. 1. $\varepsilon'_r = f(T)$ curves of samples sintered at 1200°C-2 h with MgO (wt%), having the nominal composition $K_2Sr_4(Mg_xNb_{10-x})O_{30-(3/2)x}$.

occupy the pentagonals tunnels of the TTB structure, as described in a previous study of the series $KPb_{2(1-x)}Ce_xNb_5O_{15}$.[7] Since Ta^{5+} has the same ionic radius as Nb^{5+}, it is surely present in the structure but does not effect the cell parameters. The microstructures of the corresponding sintered disks are presented in Fig. 2. They clearly show that Ta_2O_5 and ZrO_2 are efficient in improving the densification (89 and 94% of the theoretical density, respectively), unlike Sc_2O_3 and CeO_2 (71 and 64%, respectively). By SEM analysis, no secondary phases were observed in the compounds doped with Ta and Zr, whereas Sc- or Ce-rich inclusions were detected (white circles in Fig. 2), as well as a matrix largely free of these cations. Reactivity of Sc and Ce with the matrix seems to be very weak, in agreement with low densification.

The corresponding $\varepsilon'_r = f(T)$ curves are presented in Fig. 3. Low dielectric losses are observed for Ta_2O_5 and ZrO_2 in agreement with the good densifications obtained, whereas they are greater for Sc_2O_3- and CeO_2-doped samples exhibiting lower densifications. The addition of Ta_2O_5 leads to an $\varepsilon'_r = f(T)$ curve with a relatively high permittivity (>3000) and a maximum of ε'_r near 130°C. The presence of Ta^{5+} effectively decreases the T_c, which was observed near 140°C when sintered without an agent. The addition of ZrO_2 has an excellent influence on the $\varepsilon'_r = f(T)$ curve, since a maximum appears at low temperature (−30°C) and another one is visible near 70°C. The profile of this curve resembles the 'tilt' effect mentioned in the evolution of the $\varepsilon'_r = f(T)$ curves for an addition of MgO. With Sc_2O_3, the $\varepsilon'_r = f(T)$ curve exhibits a broad maximum close to 140°C. Concerning CeO_2, the curve shows a relatively constant ε'_r as a function of temperature. The action and the distribution of the cerium in the matrix seem to be more efficient than those of scandium, but the high porosity of the corresponding samples does not allow high permittivity.

3.3 $K_2Sr_{3.25}Pb_{0.75}Nb_{9.78}O_{29.45}$ sintered with ZrO_2

The partial substitution of Pb^{2+} for Sr^{2+} was performed for $K_2(Sr_{4-y}Pb_y)(Mg_xNb_{10-x})O_{30-(3/2)x}$ with $y = 0{\cdot}5$ and $0{\cdot}75$ and $x = 0{\cdot}11$ to $0{\cdot}33$. The choice of the y value was similar to the study of the Sr^{2+} - Pb^{2+} substitution in the series $K_2(Sr_{4-y}Pb_y)Nb_{10}O_{30}$, where a maximum of ε'_r appears around $y = 0{\cdot}6$.[4,5] Regardless of the x value, $\varepsilon'_r = f(T)$ curves exhibited higher permittivity when $y = 0{\cdot}75$. This value was also retained and the substitution

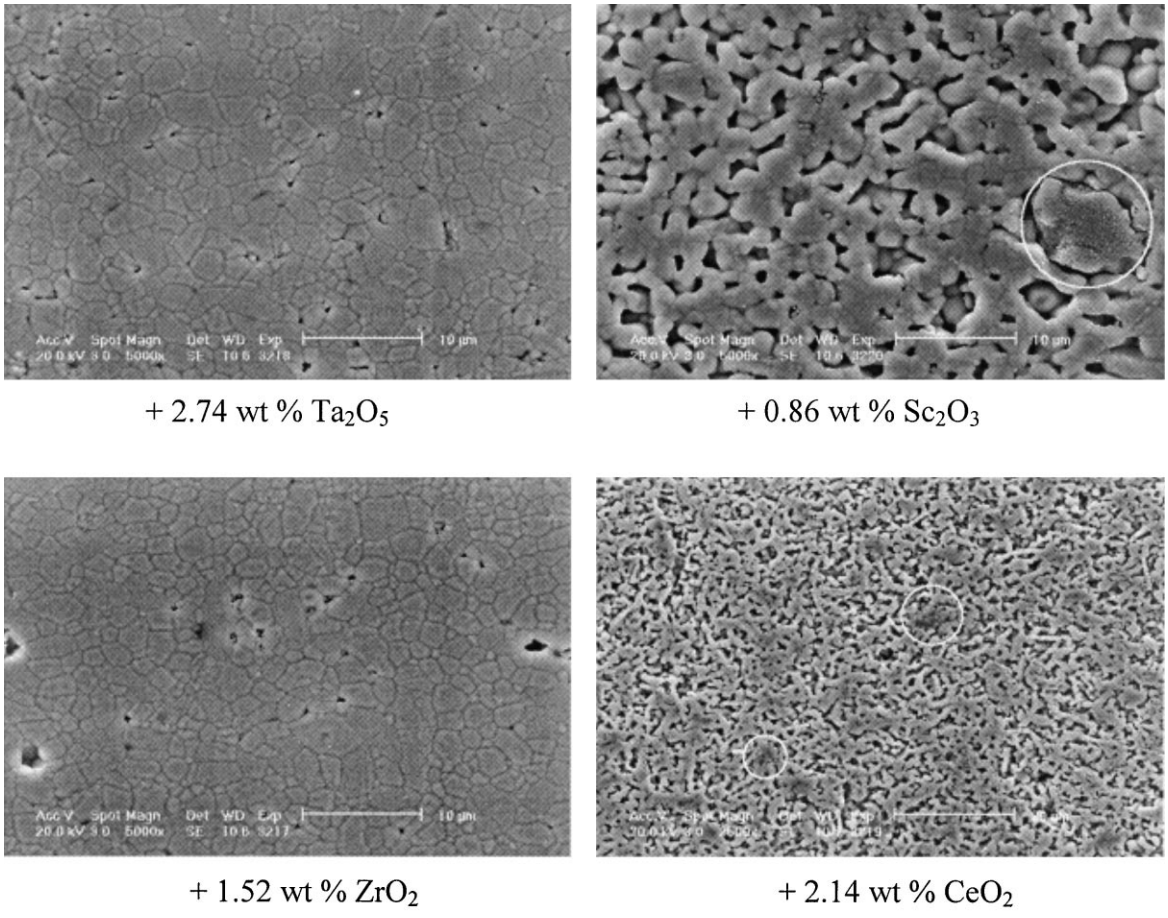

Fig. 2. Microstructures of samples sintered at 1300°C-2 h with different agents, having the nominal composition $K_2Sr_4Nb_{9.78}O_{29.45}$ (white circles indicate Sc- and Ce-rich inclusions).

of Pb^{2+} for Sr^{2+} in $K_2Sr_4Nb_{9.78}O_{29.45}$ was made according to $K_2(Sr_{3.25}Pb_{0.75})Nb_{9.78}O_{29.45}$. After sintering, the XRD pattern showed a TTB phase with strong splitting of the 620-002 lines and the density was plainly higher than that of the composition $K_2Sr_4Nb_{9.78}O_{29.45}$.

The corresponding $\varepsilon'_r = f(T)$ curve is presented in Fig. 4. The ε'_r value is high over all the temperature range (between 4000–8000) and acceptable dielectric losses are obtained (< 5%). The spread maximum as a function of temperature is certainly due to a large distribution of the cations K^+, Sr^{2+}, Pb^{2+} and vacancies in the tunnels of the TTB structure.

We have noted the efficiency of ZrO_2 as a sintering agent for the nominal composition $K_2Sr_4Nb_{9.78}O_{29.45}$, resulting in an $\varepsilon'_r = f(T)$ curve with a high permittivity and a relatively flat temperature profile,

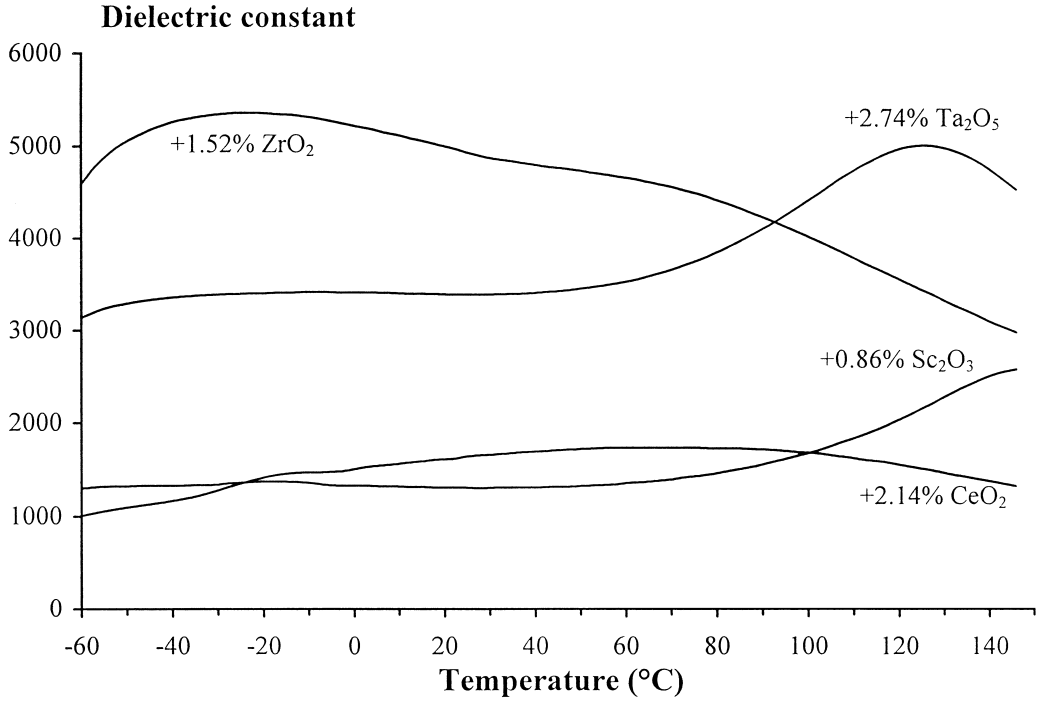

Fig. 3. $\varepsilon'_r = f(T)$ curves of samples sintered at 1300°C-2 h with different agents (wt%), having the nominal composition $K_2Sr_4Nb_{9.78}O_{29.45}$.

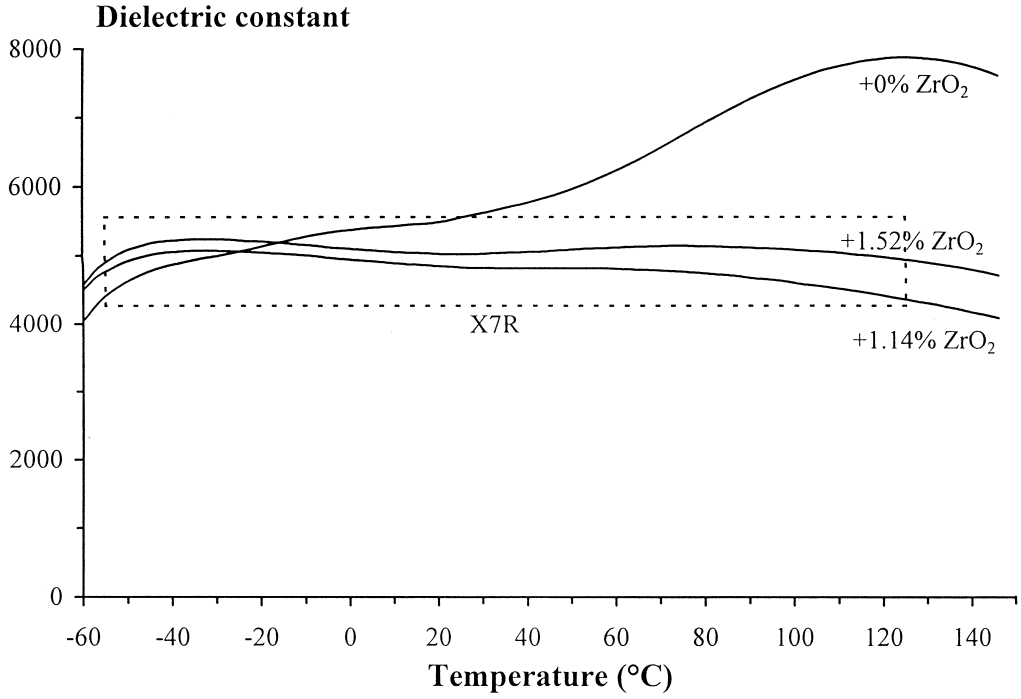

Fig. 4. $\varepsilon'_r = f(T)$ curves of samples sintered at 1300°C-2 h, without and with ZrO_2 (wt%), having the nominal composition $K_2(Sr_{3.25}Pb_{0.75})Nb_{9.78}O_{29.45}$.

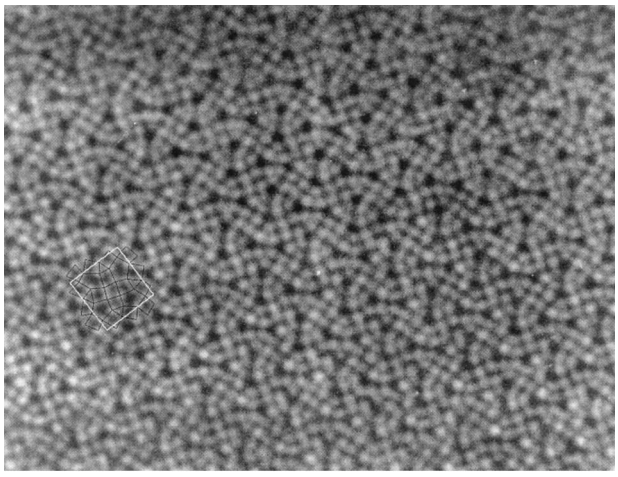

(a)

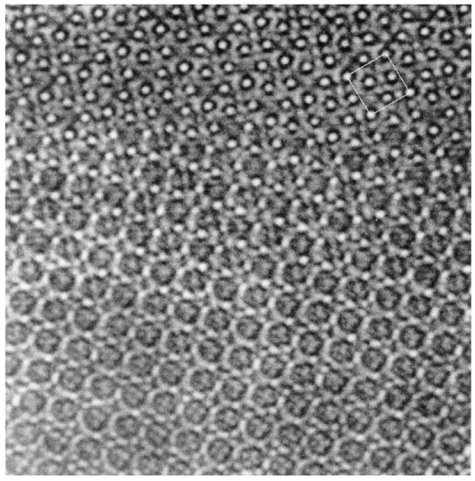

(b)

Fig. 5. [001] HREM images of the TTB phase having the nominal composition $K_2(Sr_{3.25}Pb_{0.75})Nb_{9.78}O_{29.45}$, after sintering at 1300°C-2 h with 1·14 wt% ZrO_2. (a) The white dots are correlated to the position of oxygens of the octahedral framework. (b) In the higher part of the image, the white dots are correlated to the position of cations in the pentagonal tunnels.

principally because of a maximum at low temperature. Sintering of $K_2Sr_{3.25}Pb_{0.75}Nb_{9.78}O_{29.45}$ was, therefore, carried out at 1300°C for 2 h with 1·52 and 1·14 wt% ZrO_2. No improvement of the densification is observed when ZrO_2 is added, no secondary phases are observed by SEM and only a TTB phase is detected by XRD and electron diffraction. Large grains (>100 μm) are present with some areas with micron-sized grains, but no explanation is found concerning the exaggerated grain growth. Zirconium enters easily into the TTB structure because of the remarkable effect on the $\varepsilon'_r = f(T)$ curves (Fig. 4). Indeed, both curves are compatible with the X7R specification with $\varepsilon'_{r,25°C} = 5000$. The dielectric losses are lower than 4% above −55°C.

The HREM study was performed on the compound sintered with 1·14 wt% ZrO_2. Either on a micrometric or on a nanometric scale, the regularity of the contrast of the images, along the [001] or [$\bar{1}$10] directions, confirms the formation of a complete octahedral framework with the TTB structure [Fig. 5(a)]. The occupation of the tunnels [Fig. 5(b)] and octahedral sites appears to be quasi-perfect, indicating complete disorder in the distribution of the cations. EDS analysis also displayed the constancy of the Zr/Nb and Pb/Nb ratios over each part of the cristallite. Only the Sr/K ratio shows a notable variation, from 1·5 to 3·3. An average composition was also determined to be $K_{1.76}Sr_{3.52}Pb_{0.66}Zr_{0.24}Nb_{9.78}O_{30}$ (cation ratios calculated for an O_{30} content, indicating a full occupation of A and B sites of the $A_6B_{10}O_{30}$ TTB structure). At the present time, no correlation is found between the presence of two maxima on the $\varepsilon'_r = f(T)$ curves and a structural evolution as a function of temperature. An electron diffraction study as a function of temperature could prove informative in this regard.

4 Conclusion

With $K_2Sr_4Nb_{10}O_{30}$-based compositions, excellent X7R $\varepsilon'_r = f(T)$ curves are obtained due to a single TTB phase, without the presence or the formation of a perovskite or any other phase.

ZrO_2, as a sintering agent for the nominal composition $K_2(Sr_{3.25}Pb_{0.75})Nb_{9.78}O_{29.45}$, is particularly efficient in contributing to a flat temperature profile of ε'_r. In this material, the presence of disorder, resulting from a large variation in the local K/Sr ratio and the presence of Zr on the octahedral niobium sites, is primarily responsible for the X7R $\varepsilon'_r = f(T)$ curve.

Acknowledgement

The authors are very grateful to Professor M. Hervieu for the transmission electron microscopy study and helpful discussions.

References

1. Ruan, L., Li, L. and Gui, Z., Materials in electronics. *J. Mat. Sci.*, 1997, **8**, 195–197.
2. Uchikoba, F., Ito, T. and Nakajima, S., *Jpn. J. Appl. Phys.*, 1995, **34**, 2374–2379.
3. Boufrou, B., Desgardin, G., Haussonne, J. M. and Lostec, J., *Silicates Industriels*, 1993, **7–8**, 149–160.
4. Boufrou, B., Ph.D. thesis, University of Caen, France, 1994.
5. Tribotté, B., Ph.D. thesis, University of Caen, France, 1998.
6. Ravez, J. and Pouchard, M., *Ferroelectrics*, 1997, 161–173.
7. Launay, S., *Revue de Chimie Minérale*, 1985, **22**, 749–752.